

Formation and Reactions of Alkyl, Allyl, Biallylic, and Peroxyl Radicals from Unsaturated Fatty Acids in Micellar and Monomeric Aqueous Solutions

Mohamad Al-Sheikhly,* Joseph Silverman, Michael Simic, and Barry Michael

Department of Materials Science and Engineering, University of Maryland,
College Park, Maryland 20742-2115

Received: May 25, 2004; In Final Form: August 18, 2004

Pulsed irradiation experiments with spectrophotometric and conductivity detection were performed on aqueous solutions of unsaturated fatty acids in monomeric form and as rod-shaped micelles. The initial $\bullet\text{OH}$ and $\text{O}^{\bullet-}$ radicals produce allylic and biallylic free radicals as well as $\bullet\text{OH}$ adducts. The reactions of these radicals and their corresponding peroxyl radicals were investigated. The rate constant for the reaction of $\bullet\text{OH}$ with linoleate is $1 \times 10^{10} \text{ L mol}^{-1} \text{ s}^{-1}$ for the monomeric form and $3.7 \times 10^8 \text{ L mol}^{-1} \text{ s}^{-1}$ for the rod-shaped micelle, with a sharp decrease occurring as increasing linoleate content nears its critical micelle concentration. The rate constant of $\text{O}^{\bullet-}$ radicals is lower, $k = 1.6 \times 10^9 \text{ L mol}^{-1} \text{ s}^{-1}$ in dilute solutions, decreasing to $1.0 \times 10^8 \text{ L mol}^{-1} \text{ s}^{-1}$ at 10 mmol L^{-1} linoleate, where rod-shaped micelles start forming. Though $\bullet\text{OH}$ radicals form $\bullet\text{OH}$ adducts, alkyl, allyl, and biallylic radicals, $\text{O}^{\bullet-}$ radicals form a selective group of allylic and biallylic radicals. The biallylic radicals are also produced as a result of abstraction of hydrogen atoms from the linoleate by the linoleate $\bullet\text{OH}$ adducts and by alkyl radicals; this process is enhanced in the rod-shaped micelles. The yield of biallylic radicals increases with increasing micellation and with decreasing dose rate. The peroxyl radicals derived from the OH adducts of linoleate, linolenate, and arachidonate undergo unimolecular elimination of hydroperoxide (HO_2^{\bullet}) or superoxide ($\text{O}_2^{\bullet-}$). The yield of $\text{HO}_2^{\bullet}/\text{O}_2^{\bullet-}$ increases with the increasing number of double bonds.

Introduction

Ionizing radiation-induced effects on lipids and their subunits, the fatty acids, are essential in radiation biology, because they are the building blocks of the cell membrane. Radiation-induced oxidation of lipids and lipid–protein complexes such as lipoproteins plays an important role in the radiation biology of the cell. Aqueous and micellar systems of linoleates, in particular, and other fatty acids (LH_2) such as linolenic, arachidonic, and oleic acids, have been used frequently as models in the studies of radiation effects on lipids in particular, and cell membranes in general.¹ In linoleic, linolenic, and arachidonic acids, the most sensitive sites are the biallylic positions between two double bonds at (C11), (C11, C14), and (C7, C10, C13), respectively. These sites are subject to hydrogen abstraction reactions by the peroxyl radicals (ROO^{\bullet}) after which they can initiate chain reactions



Like other C-centered radicals, unsaturated fatty acid free radicals ($\bullet\text{LH}$) react rapidly with the molecular oxygen, giving rise to the formation of the fatty acid peroxyl radicals.^{2,3} Due to the resonance nature of the biallylic radicals formed in unsaturated fatty acids, oxygen adds to two of their canonical mesomeric sites, yielding two from the allylic and three from the biallylic isomeric peroxyl radicals.⁴ In the radiolysis of the aqueous monomeric and micellar systems, fatty acids peroxyl radicals undergo various reactions, which depend on dose-rate (D_r), initial fatty acid concentrations, and the chemical structures.

These include bimolecular reactions forming the tetroxides intermediates, abstraction of biallylic H-atoms from other fatty acid molecules initiating chain reactions, and intramolecular addition of the peroxyl radical to a neighboring double bond.^{5–7}

In this work, using spectrophotometric and conductometric pulse radiolysis methods, previously published kinetics studies of the carbon-centered radicals⁴ were extended to cover the radicals formed in aqueous and rod-shaped micellar systems of unsaturated fatty acids, in the absence and presence of oxygen. In addition to the well-known bimolecular decay reactions and abstraction reaction of biallylic hydrogen from a neighboring unsaturated fatty acid molecule, this work also demonstrates that the peroxyl radicals of the unsaturated fatty acid $\bullet\text{OH}$ adducts in aqueous solutions undergo unimolecular hydroperoxide (HO_2^{\bullet}) or superoxide elimination ($\text{O}_2^{\bullet-}$) reactions.

Experimental Section

Kinetics of transient species, as determined from their UV–vis spectra, and conductivity, were measured by the methods and procedures of the National Institute of Standards and Technology (NIST) and the Gray Laboratory.^{8,9} Radiolysis of aqueous solutions by high-energy electrons generates $\bullet\text{OH}$ ($2.9 \times 10^{-7} \text{ mol J}^{-1}$), hydrated electrons, (e_{aq}^-) ($2.9 \times 10^{-7} \text{ mol J}^{-1}$), and H-atoms ($0.6 \times 10^{-7} \text{ mol J}^{-1}$). The yield of the $\bullet\text{OH}$, in aqueous solutions saturated with N_2O is enhanced by virtue of the conversion of e_{aq}^- to $\bullet\text{OH}$ [$\text{N}_2\text{O} + e_{\text{aq}}^- \rightarrow \bullet\text{OH} + \text{N}_2 + \text{OH}^-$]. Hence the predominant radical species initially produced in such solutions is $\bullet\text{OH}$ ($5.8 \times 10^{-7} \text{ mol J}^{-1}$) accompanied by a much lower yield of $\bullet\text{H}$ ($0.6 \times 10^{-7} \text{ mol J}^{-1}$),

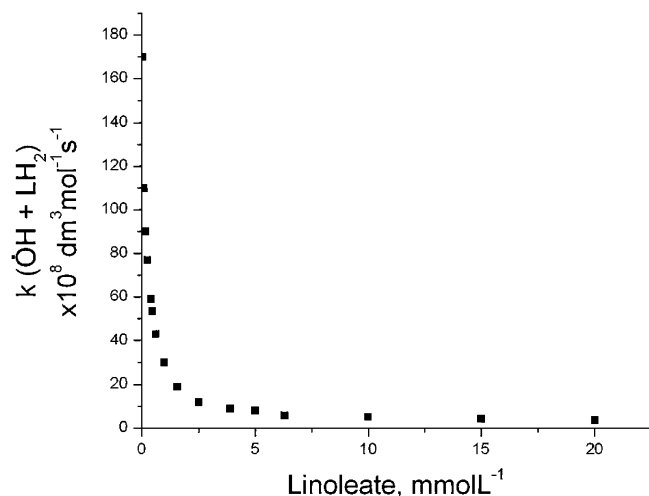


Figure 1. Effect of linoleate concentration on the reaction rate constants of the $\bullet\text{OH}$ radicals with the linoleate in the pulsed N_2O -saturated aqueous solutions of linoleate acid. Dose rate: 18.5–19 Gy per 20 ns pulse. pH = 11.

where the numbers in parentheses indicate their G values in SI units (mol J^{-1}). Of particular interest in this work are the $\bullet\text{OH}$ reactions with unsaturated fatty acids, the nature of the radical species formed thereby, and subsequent reactions of these species.

Oleic, linoleic, linolenic, and arachidonic acids and their sodium salts (Sigma) were used without further purification because their peroxidation levels were negligible. N_2O and O_2 were mixed in desired ratios before they were introduced into aqueous solutions; $[\text{O}_2]$ was measured by a standard Clark oxygen electrode (Orion).

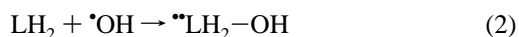
Rate constants for reactions of $\bullet\text{OH}$ radicals with aqueous and micellar forms of linoleate¹¹ were determined by competition kinetics using carbonate as the reference reactant. The reaction of $\bullet\text{OH}$ radicals with carbonate produces $\text{CO}_3^{\bullet-}$ radical ions ($\lambda_{\text{max}} = 600 \text{ nm}$, $\epsilon = 1900 \text{ L mol}^{-1} \text{ cm}^{-1}$), which are fairly long-lived. All experiments were carried out at pH 11 and the rate constant for the carbonate/bicarbonate mixture at this pH was assumed to be $3.6 \times 10^8 \text{ L mol}^{-1} \text{ s}^{-1}$.¹² For measuring dose per pulse, the SCN^- method was used.¹³

Results and Discussion

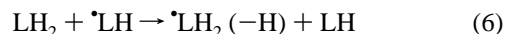
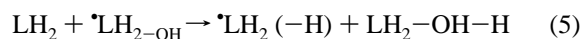
In the Absence of Oxygen. The overall reaction rate constants of $\bullet\text{OH}$ with monomeric and micellar systems of linoleate were measured using the carbonate competition method.¹⁰ Figure 1 shows the effect of linoleate concentration on the overall reaction rate constants of $\bullet\text{OH}$ with monomeric and micellar structures in N_2O -saturated solutions. As expected, there is a change in its value ($(1 \pm 0.2) \times 10^{10} \text{ L mol}^{-1} \text{ s}^{-1}$) at concentrations below the critical micelle concentration ($\text{cmc} = 2.3 \text{ mmol L}^{-1}$). This value agrees fairly well with the previous published value.¹⁴ Below the cmc, the linoleate is mostly present in monomeric form. As the linoleate concentration increases, the reaction rate constant decreases, notably as the concentration reaches 2–3 mmol L^{-1} . Above this concentration, the micellar structure becomes predominant and $\bullet\text{OH}$ radicals react with micelles in preference to the monomers. The reason is that the higher concentration of structural units in micelles dominates the higher reactivity of free monomer units. The reactivity effect is expected because the aggregation can lower the observed rate constant. The spherical micelles, which form just above the cmc assume a rod-shaped micellar structure at concentrations beyond

12 mmol L^{-1} LH_2 .^{15,16} The overall reaction rate constants decrease from $(1 \pm 0.2) \times 10^{10} \text{ L mol}^{-1} \text{ s}^{-1}$ in the 0.1–1 mmol L^{-1} concentration range (monomeric) to $(3.7 \pm 0.7) \times 10^8 \text{ L mol}^{-1} \text{ s}^{-1}$ at 20 mmol L^{-1} (rod-shaped micelle).

We also used optical pulse radiolysis to measure directly the reaction rate constant for the reaction of $\bullet\text{OH}$ with the rod-shaped micelle linoleate molecules. The experiments were carried out in N_2O -saturated solutions containing 10–20 mmol L^{-1} linoleate at pH = 9.7–10.2. There are two relevant reactions: abstraction of the H from CH_2 groups along the chain, and addition to the double bonds. The $\bullet\text{OH}$ can abstract a hydrogen atom from the biallic position producing a free radical that absorbs at $\lambda_{\text{max}} = 282\text{--}284 \text{ nm}$.¹⁷ Figure 2a shows the buildup of the linoleate free radicals transient spectra of pulsed N_2O -saturated 20 mmol L^{-1} sodium linoleate at pH 10.7. The buildup at 280 nm has two components: a fast component that is complete within 30 μs after the pulse, followed by a comparatively slower component that reaches a plateau at 300 μs . Figure 2b shows the transient optical spectra at 30 and 300 μs . Though the spectrum at 30 μs is broad and weak with a molar absorption coefficient of $1.65 \times 10^3 \text{ L mol}^{-1} \text{ cm}^{-1}$, the spectrum at 300 μs is strong with a sharp absorption at 280 nm and a molar absorption coefficient of $4.3 \times 10^3 \text{ L mol}^{-1} \text{ cm}^{-1}$, assuming the $G(\bullet\text{OH} + \bullet\text{H}) = 6.4 \times 10^{-7} \text{ mol J}^{-1}$. The initial reactions of $\bullet\text{OH}$ with linoleate, which is represented by the fast component, are expected to be (1) the addition to double bonds producing $\bullet\text{OH}$ adduct free radicals $\bullet\text{LH}_2\text{--OH}$, (2) abstraction of the hydrogen atom from C–H bonds along the chain, giving rise to alkyl ($\bullet\text{LH}$), and (3) abstraction of hydrogen atoms from the biallic positions to form biallic radicals ($\bullet\text{LH}_2\text{--(H)}$)



Addition of $\bullet\text{OH}$ to the double bonds of the linoleate is a much more rapid reaction than either of the two abstraction reactions [(4), (5)].^{1,12} Hence the transient optical spectrum at 30 μs represents the $\bullet\text{LH}_2\text{--OH}$ radical primarily along with a small contribution from $\bullet\text{LH}$ and $\bullet\text{LH}_2\text{--(H)}$ radicals. The slower buildup at 280 nm has already been reported and is attributed to reactions 5 and 6,¹³ producing biallic free radicals. Figure 3 shows the effects of dose rate and the initial linoleate concentration on the absorbance at 280 nm (i.e., biallic free radical yield): as the concentration of the initial linoleate increases $[\text{LH}_2]$, the yield at 280 nm increases; but, as the dose rate increases, the yield decreases. It is very well-known that biallic carbon-centered free radicals have rather strong absorption around 280 nm.¹² Hence it is likely that the results in Figure 3 are due to the formation of linoleate biallic free radicals by abstraction of hydrogen atoms from linoleate molecules by $\bullet\text{LH}_2\text{--OH}$ and $\bullet\text{LH}$ radicals.



On the basis of this model, increasing the linoleate concentration enhances reactions 5 and 6, thereby increasing the formation of biallic radicals. To test the model, rate data for biallic radical concentration were obtained as a function of linoleate concentration and dose per pulse. They show (Figure 4) a pseudo-first-order increase of $\bullet\text{LH}_2\text{--(H)}$ with time. This is

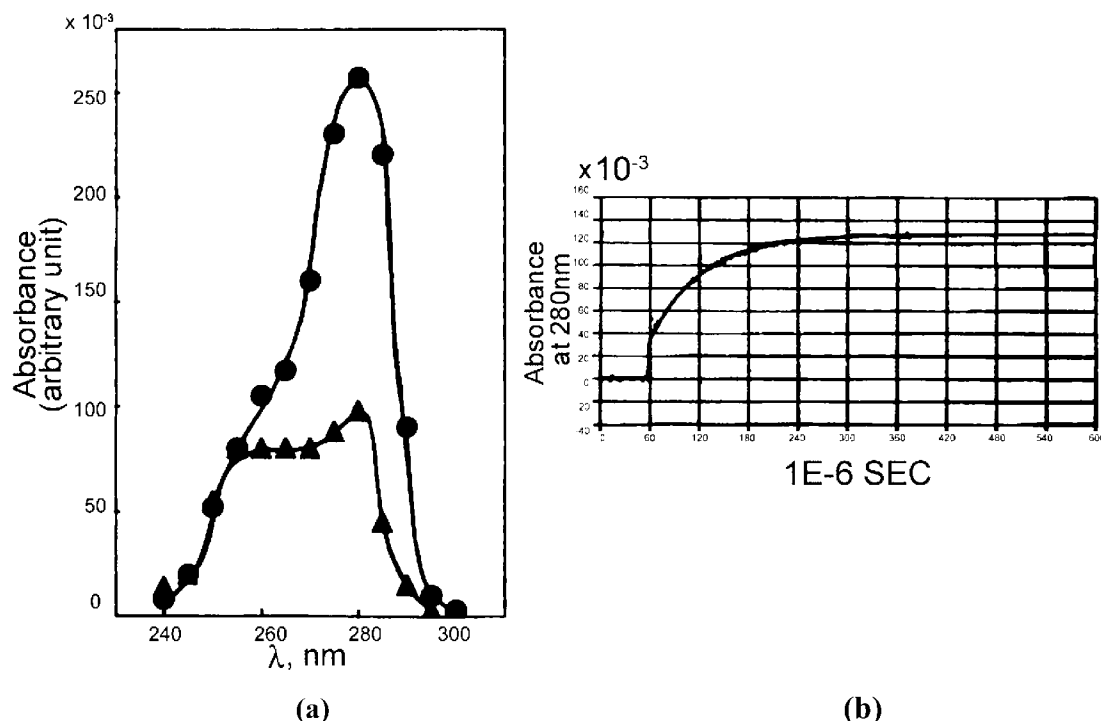


Figure 2. (a) Transient spectra of the pulsed irradiated N_2O -saturated rod-shaped micellar aqueous solutions 20 mmol L^{-1} at 30 and $300 \mu\text{s}$ after the pulse. Dose rate: $100 \text{ Gy per } 20 \text{ ns pulse}$. $\text{pH} = 10.7$ (b) Fast and slow buildup at 280 nm in the pulsed irradiated N_2O -saturated solutions of rod-shaped micellar aqueous solutions 20 mmol L^{-1} , $\text{pH} = 10.7$.

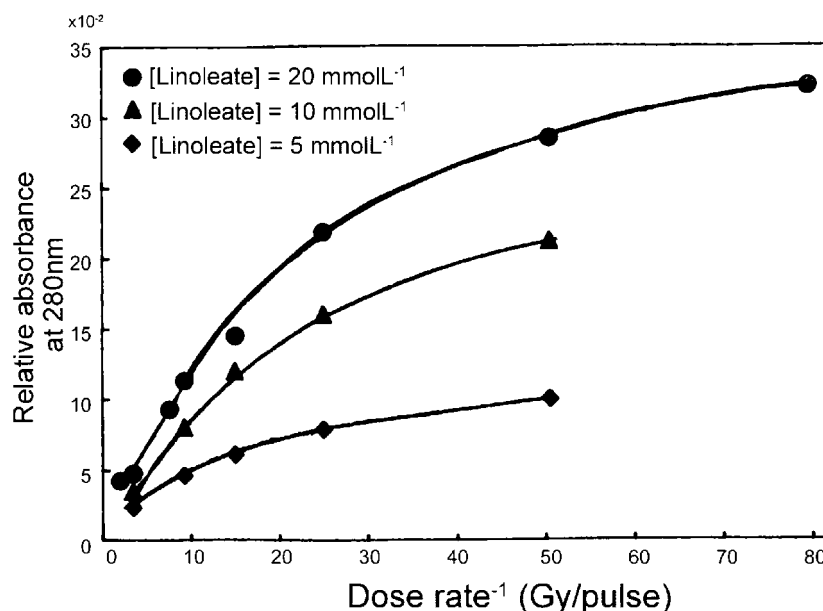
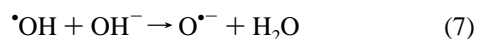


Figure 3. Effect of the dose rate on the yield of bialkyl radicals at 280 nm in the pulsed irradiated N_2O -saturated solutions of linoleate at 5 , 10 , and 20 mmol L^{-1} concentrations.

consistent with the model provided that radical–radical reactions are assumed to be relatively slow in the range of our experimental conditions.

Direct abstraction of bialkyl hydrogen from monomers and micelles was achieved using oxide monoion radicals ($\text{O}^{\bullet-}$) rather than $\bullet\text{OH}$. $\text{O}^{\bullet-}$ is considered very selective for abstracting bialkyl hydrogen atom.^{12,18,19} In pulsed N_2O -saturated solutions of 0.5 mmol L^{-1} linoleate at $\text{pH} \sim 13.5$, $[\text{KOH}] = 0.7 \text{ mol L}^{-1}$, the $\bullet\text{OH}$ radicals are converted to $\text{O}^{\bullet-}$:



which $\text{O}^{\bullet-}$ abstract H atoms from the bialkyl position of

linoleate micelles, thereby producing the bialkyl radicals

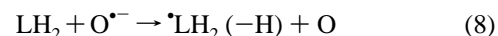


Figure 5 shows the transient spectrum of the bialkyl radicals $\bullet\text{LH}_2 (-\text{H})$ in the N_2O -saturated solution of linoleate at $\text{pH} \sim 13.5$. There are two noteworthy absorption bands: the one at $\sim 280 \text{ nm}$ ($\epsilon_{275-282} = 4 \times 10^3 \text{ L mol}^{-1} \text{ cm}^{-1}$, assuming the $G(\bullet\text{OH}) = 5.8 \times 10^{-7} \text{ mol J}^{-1}$, which is related to $\bullet\text{LH}_2 (-\text{H})$) and a shoulder at $\sim 250 \text{ nm}$ indicating the production of the alkyl radicals. The production of the alkyl radicals can be attributed to the addition of the remaining fraction of $\bullet\text{OH}$ to the linoleate, because at $\text{pH} \sim 13.5$, $\sim 3\%$ $\bullet\text{OH}$ radicals still

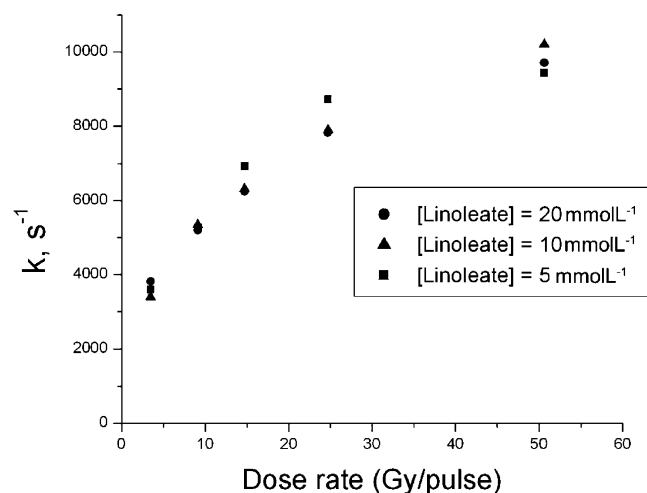


Figure 4. Dose rate dependence of the pseudo-first-order buildup of the formation reaction of the biallylic radicals in the pulsed irradiated N_2O -saturated solutions of linoleate at 5, 10, and 20 mmol L^{-1} concentrations.

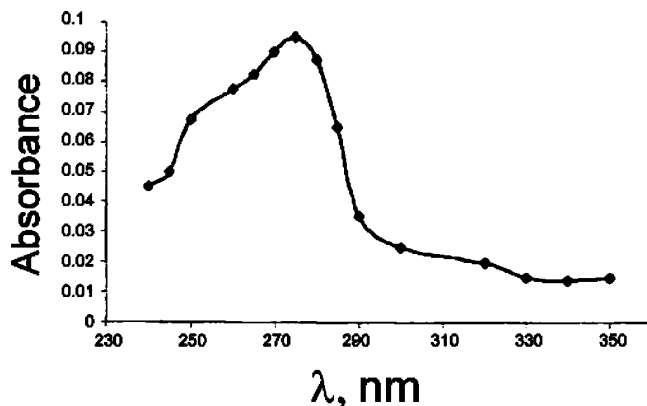
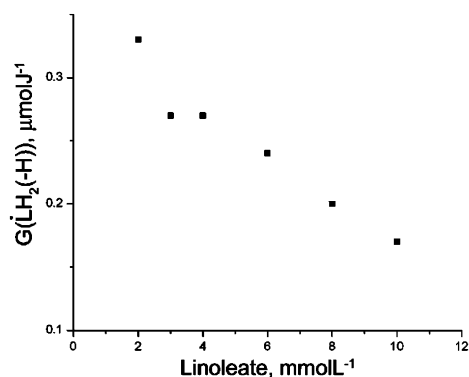


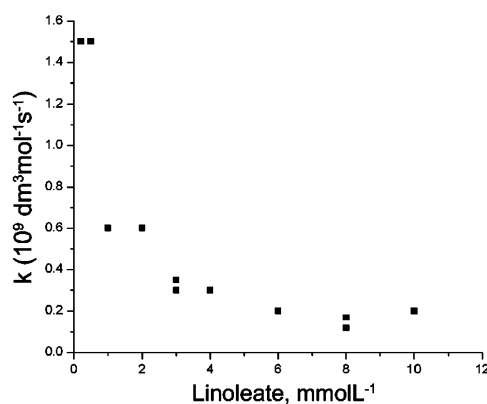
Figure 5. Transient absorption spectrum of biallylic radical in the pulsed irradiated N_2O -saturated solutions of 0.5 mmol L^{-1} linoleate + 0.7 M KOH, pH ~ 13.5 . Dose rate: 42 Gy per 20 ns pulse.

remain in the solutions. In addition, because the reaction rate constant of $\cdot\text{OH}$ with linoleate is $(1 \pm 0.2) \times 10^{10} \text{ L mol}^{-1} \text{ s}^{-1}$ compared to $(2.5 \pm 0.4) \times 10^9 \text{ L mol}^{-1} \text{ s}^{-1}$ of $\text{O}^{\cdot-}$ with linoleate, one would expect that the yield of the reaction of $\cdot\text{OH}$ with linoleate is at least 12% of the yield of the $\text{O}^{\cdot-}$ reaction with the linoleate. These considerations account for the considerable yield of alkyl radicals even at pH ~ 13.5 . In addition to the abstraction of biallylic hydrogen, the reaction of $\text{O}^{\cdot-}$ with linoleate also includes abstraction of alkyl and allylic hydrogen. Figure 6a shows the dependence of the biallylic radical yield, $G(\cdot\text{LH}_2(-\text{H}))$, as a function of the linoleate concentration. As the micelles start forming by increasing the linoleate concentration, $G(\cdot\text{LH}_2(-\text{H}))$ decreases, suggesting less reaction of $\text{O}^{\cdot-}$ with the linoleate. These results are related to the drop in pH by several units at the electrical double-layer near the micelle surface,²⁰ where $\text{O}^{\cdot-}$ is scavenged through the $\text{O}^{\cdot-} + \text{H}^+ \rightarrow \cdot\text{OH}$ reaction. The repulsion between the negative $\text{O}^{\cdot-}$ and the negative carboxylic groups also contributes to this decrease in $\text{O}^{\cdot-}$ reactivity. Also, one would expect, as in the case of the reaction of $\cdot\text{OH}$ with linoleate, that the more complex the structure of the micelle, the less is the accessibility of the allylic structure to $\text{O}^{\cdot-}$. Furthermore, as expected, Figure 6b shows the decrease in the reaction rate constant of $\text{O}^{\cdot-}$ with linoleate as the [linoleate] increases.

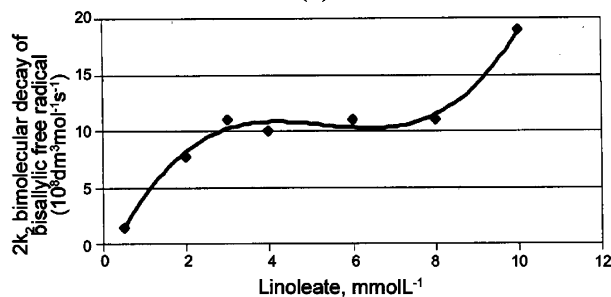
To investigate the effect of the degree of micelle structure on the bimolecular decays ($2k_2$) of the biallylic radicals, their



(a)



(b)



(c)

Figure 6. Effect of linoleate concentration on (a) $G(\cdot\text{LH}_2(-\text{H}))$, (b) the reaction rate constants of $\text{O}^{\cdot-}$ with linoleate, and (c) the bimolecular decay rate constants of the biallylic radical in the pulsed irradiated N_2O -saturated solutions of linoleate + 0.7 M KOH, pH ~ 13.5 .

values were measured as a function of linoleate concentration by monitoring the decay at 280 nm in pulse-irradiated N_2O -saturated solutions of various concentrations of linoleate at pH ~ 13.5 . Figure 6c shows that in the region 0.05–3 mmol L^{-1} , as the linoleate concentration increases, formation of micelles becomes pronounced at the cmc, and the bimolecular decay constants increase. The increase in $2k_2$ is indicative of the formation of more than one free radical within the dimers, trimers, and the spherical micelle. Around 3 mmol L^{-1} concentrations, the decay rates reach a plateau. Despite the fact that as the concentration increases from 3 to 8 mmol L^{-1} , whereby the micelles reach greater structural organization and a higher number of LH_2 molecules per micelle unit, a plateau of bimolecular decay constants was measured. The same plateau was previously observed in this region, in the O_2 -uptake experiments,⁴ and attributed to the open-ended self-association reaction.⁴ This means that the linoleate molecules undergo self-

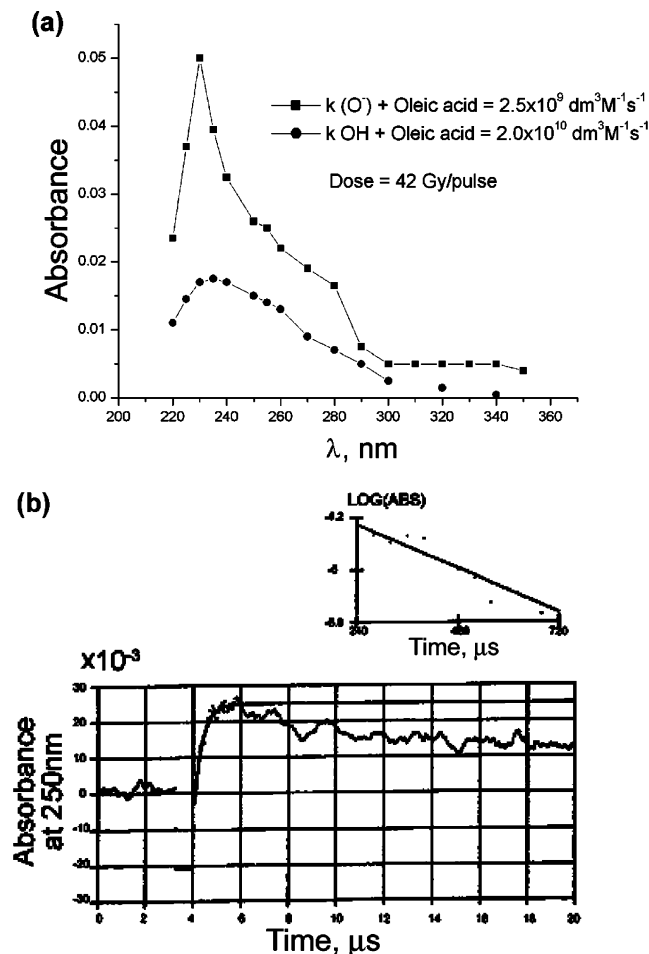
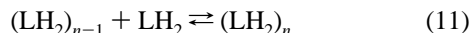
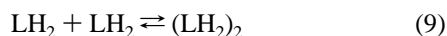


Figure 7. (a) Absorption spectra of alkyl and allylic radicals formed by pulse radiolysis of N_2O -saturated solutions of 0.05 mmol L^{-1} oleate: alkyl radicals, natural pH; allyl radicals, pH ~ 13.5 ; 0.7 M KOH . (b) Pseudo-first-order buildup at 250 nm of the alkyl radical in the pulsed irradiated N_2O -saturated solutions of oleic acid at natural pH.

assembly through the aggregation so that the concentration of the reactive species is not proportional to the overall linoleate concentration.

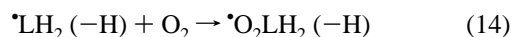
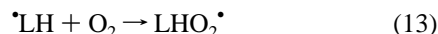


A comparison was made between the linoleate and oleate free radicals, as observed in the pulse radiolysis experiments. Figure 7a shows two transient spectra. The top one is attributed almost entirely to allylic radicals formed at pH ~ 13.5 by the reaction of $\text{O}^{\bullet-}$ with oleate; the bottom one is due mainly to alkyl radicals formed by $\bullet\text{OH}$ reaction with oleate at natural pH. These spectra contain some contributions from alkyl radicals formed from $\text{O}^{\bullet-}$ reactions and allyl radicals produced by $\bullet\text{OH}$ reactions.

The molar absorption coefficient of the oleate alkyl and allylic radicals were found to be $\sim 0.7 \times 10^3$ and $\sim 2 \times 10^3 \text{ L mol}^{-1} \text{ cm}^{-1}$, respectively. The reaction rate constants of $\bullet\text{OH}$ and $\text{O}^{\bullet-}$ with oleate acid were found to be $(1.8 \pm 0.3) \times 10^{10}$ and $(2.5 \pm 0.4) \times 10^9 \text{ L mol}^{-1} \text{ s}^{-1}$, respectively. As shown in Figure 7b, the absence of the slower buildup in the case of oleate, in

contrast with the case of linoleate, strongly suggests that unlike the linoleate alkyl radicals, the oleate alkyl radicals do not abstract another H atom from a neighboring oleate molecule because of the lack of biallylic positions in the oleate molecule. The pseudo first-order buildup at 232 nm represents the abstraction of alkyl hydrogen by $\text{O}^{\bullet-}$. Both alkyl and allyl radicals decay bimolecularly with reaction rate constants, $2k_2$, $(1 \pm 0.15) \times 10^9$ and $(1.6 \pm 0.24) \times 10^9 \text{ L mol}^{-1} \text{ s}^{-1}$, respectively.

In the presence of Oxygen. As expected, in the radiolysis of $\text{N}_2\text{O}/\text{O}_2$ -saturated aqueous solution of linoleate, the $\bullet\text{OH}$ adduct peroxy radicals ($\bullet\text{O}_2\text{LH}_2\text{-OH}$), alkyl peroxy radicals (LHO_2^\bullet), and biallylic peroxy radicals are formed:



The overall reaction rate constant of the addition of molecular oxygen to these radicals ($\bullet\text{LH}_2\text{-OH}$, $\bullet\text{LH}$, and $\bullet\text{LH}_2(-\text{H})$) was measured by monitoring the pseudo first-order decay at 280 nm as a function of $[\text{O}_2]$ (The range of $[\text{O}_2]$ was $0.07\text{--}0.26 \text{ mmol L}^{-1}$) and found to be $(1.8 \pm 0.3) \times 10^8 \text{ L mol}^{-1} \text{ s}^{-1}$ in the pulsed irradiated $\text{N}_2\text{O}/\text{O}_2$ -saturated aqueous solutions of 1 mmol L^{-1} at pH ~ 9.4 . This value is comparatively much less than the rate constants for reactions of alkyl radicals with oxygen, which are around 10^9 to $10^{10} \text{ L mol}^{-1} \text{ s}^{-1}$.¹ However, it is comparable to the reaction rate constant of oxygen with the hydroxycyclohexadienyl radicals, which is $3.5 \times 10^8 \text{ L mol}^{-1} \text{ s}^{-1}$.²¹

Optical pulse radiolysis experiments were carried out to measure the spectra of the alkyl and biallylic linoleate peroxy radicals. Figure 8a shows the recorded transient spectrum of linoleate peroxy radicals at 0.1 ms after the pulse in ($50\% \text{ N}_2\text{O} + 50\% \text{ O}_2$)-saturated aqueous solutions of 0.1 mmol L^{-1} linoleate at pH = 9.3; the 14.8 Gy dose in 20 ns pulse gives rise to a maximum absorption at 245 nm with $\epsilon_{245} = 1200 \text{ L mol}^{-1} \text{ cm}^{-1}$. The spectrum was corrected for the small contribution of $\text{O}_2^{\bullet-}$ ($G(\text{O}_2^{\bullet-}) = 0.062 \mu\text{mol J}^{-1}$), which is a result of reaction $\bullet\text{H} + \text{O}_2 \rightarrow \text{HO}_2^\bullet/\text{O}_2^{\bullet-}$. Nearly 90% of the absorbance is due to the nonallylic and monoallylic peroxy radicals and 10% is accounted for by biallylic peroxy radicals, because the biallylic radicals formed by $\bullet\text{OH}$ are only 10% of the total radical yield. Figure 8b represents the biallylic linoleate peroxy radical transient spectrum in the pulsed ($50\% \text{ N}_2\text{O} + 50\% \text{ O}_2$)-saturated aqueous solutions of 0.1 mmol L^{-1} linoleate, at pH ~ 13 and a dose rate of 17 Gy/pulse with $\epsilon_{245} = 3770 \text{ L mol}^{-1} \text{ cm}^{-1}$. In addition to this increase in the value of ϵ_{245} , the spectrum has a shoulder around 280 nm , which is attributed to the conjugated nature of the system.

It has already been reported that in the radiolysis of oxygenated aqueous solutions of some organic compounds, the $\bullet\text{OH}$ adduct peroxy radicals undergo HO_2^\bullet or $\text{O}_2^{\bullet-}$ unimolecular elimination reactions, which depend on dose rate, pH, and buffer concentrations.^{22–24} Likewise, the peroxy radicals derived from the $\bullet\text{OH}$ adduct of benzene also undergo unimolecular HO_2^\bullet and $\text{O}_2^{\bullet-}$ elimination.²⁵

The reactivity of the linoleate peroxy radicals was followed at 245 nm , at the lowest possible dose rate ($10\text{--}14 \text{ Gy/pulse}$) to enhance the first-order decay relative to the bimolecular decay of the linoleate peroxy radicals. The buildup at 245 nm exhibits pseudo-first-order behavior, as shown in Figure 9a, which

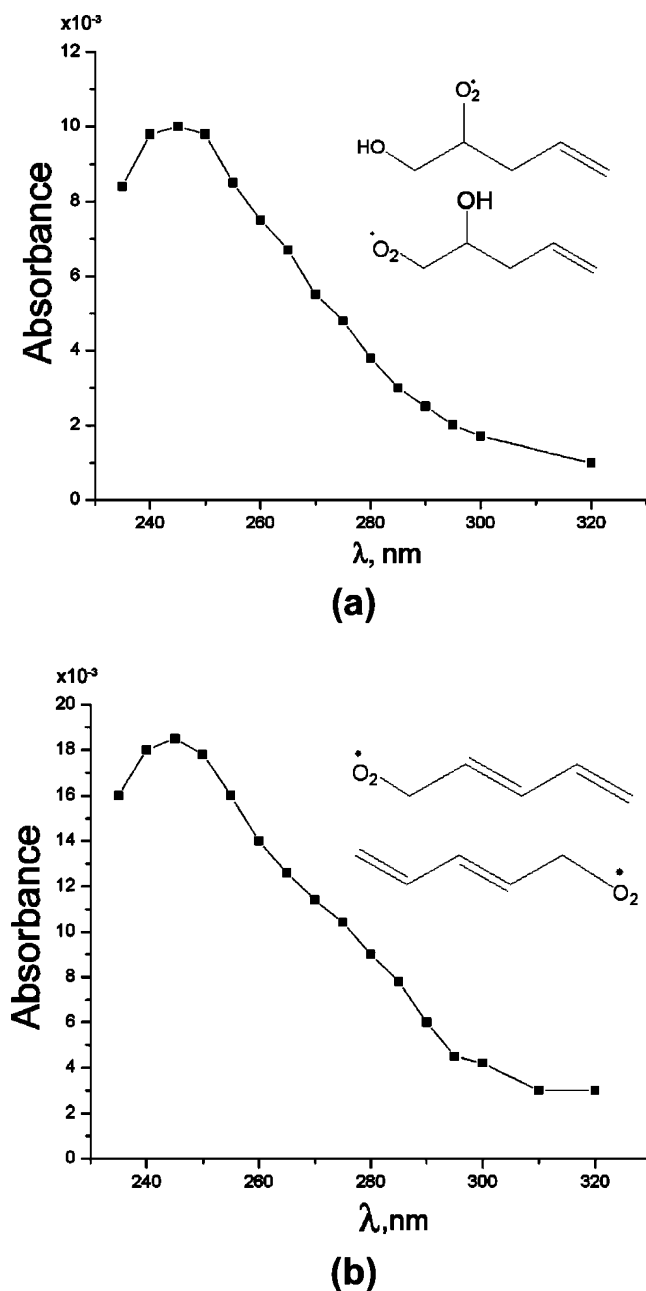


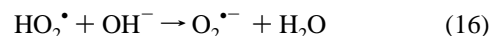
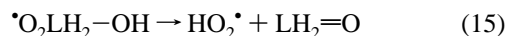
Figure 8. (a) Absorption transient spectrum of the alkyl peroxy radical at 0.1 ms after the pulse of the linoleate peroxy radicals in pulsed (50% N₂O + 50% O₂)-saturated aqueous solutions of 0.1 mmol L⁻¹ linoleate, at pH = 9.3 and dose rate of 14.8 Gy/pulse. (b) Absorption transient spectrum of the bialkyl linoleate peroxy in the pulsed irradiated (50% N₂O + 50% O₂)-saturated aqueous solutions of 0.1 mmol L⁻¹ linoleate, at pH ~ 13. Dose rate: 17 Gy/pulse.

represents the production of O₂^{•-}. This judgment is based on the fact that its molar absorption coefficient at 245 nm is 2350 L mol⁻¹ cm⁻¹, compared with 1200 M⁻¹ cm⁻¹ for the peroxy radical. The measurements were carried out in the pH range 8.5–11. At pH = 8.5–9.3, the reaction rate constant is $(4 \pm 0.6) \times 10^4$ s⁻¹. At pH ~ 7.5, there is no observable buildup at 245 nm, suggesting that the O₂^{•-} elimination is a base-catalyzed reaction. It should be mentioned that the turbidity of linoleate aqueous solutions below pH 7.5 prevents optical measurements in more acid conditions. The pseudo-first-order buildup at 245 nm is followed by second-order decay with the value of $2k_t = (2.4 \pm 0.4) \times 10^7$ L mol⁻¹ s⁻¹ at 0.1 mmol L⁻¹ linoleate.⁴ At pH ~ 13, where mainly bialkyl peroxy radicals of the linoleate

are produced, the bimolecular decay constant is $(6-7) \times 10^6$ L mol⁻¹ s⁻¹ in the pulsed irradiated aqueous solutions of 0.1 mmol L⁻¹ linoleate. However, at pH ~ 10.3, as the concentration of linoleate increases, the bimolecular decay of the linoleate peroxy radicals decreases. At 20 mmol L⁻¹ linoleate concentration, no decay was observed for at least 4 ms, indicating that in rod-shaped micelles, peroxy radicals undergo intramolecular H-abstraction within single micelles.

Elimination of O₂^{•-} can also be observed by using pulse radiolysis with conductivity detection.²⁶ Figure 9b shows the conductivity of pulsed irradiated (50% N₂O + 50% O₂)-saturated solutions of 0.1 mmol L⁻¹ linoleate at pH ~ 10. Similar to most pulsed conductivity measurements in aqueous solutions, there is a sharp increase (less than 0.2 μs) in the conductivity due to the formation of H₃O⁺ ($\lambda^\circ = 315 \Omega^{-1} \text{ cm}^2 \text{ mol}^{-1}$) and OH⁻ ($\lambda^\circ = 170 \Omega^{-1} \text{ cm}^2 \text{ mol}^{-1}$). This sharp increase in conductivity is followed by two first-order decay processes.

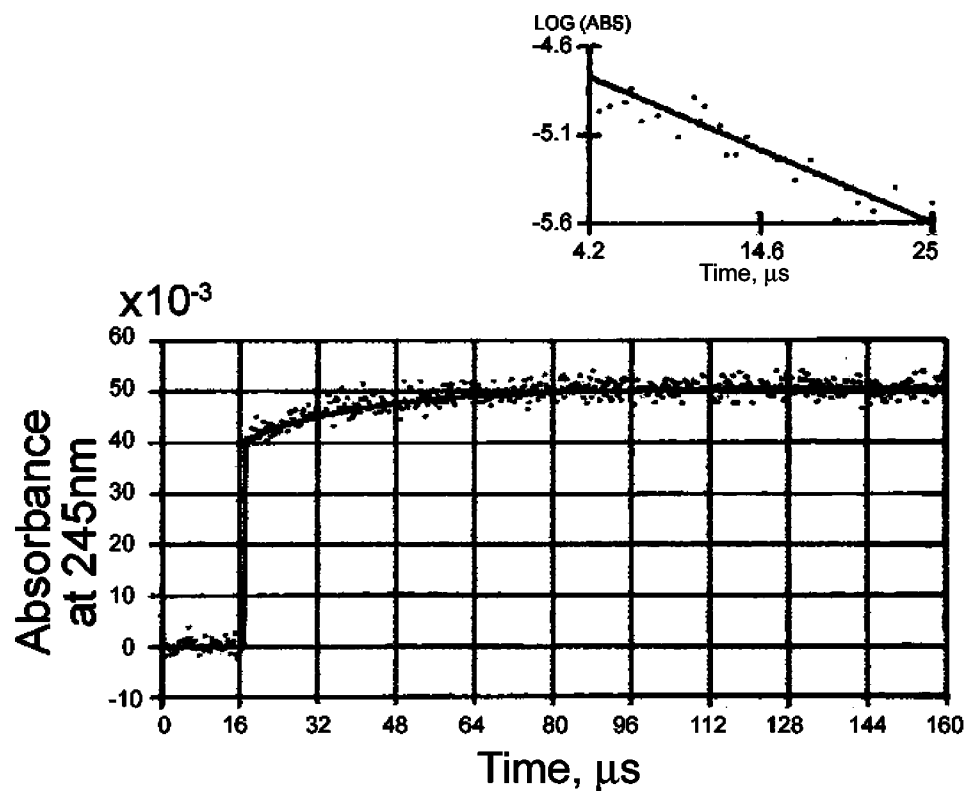
The first conductivity decay is comparatively fast with observed reaction rate constants of $(3.8 \pm 0.6) \times 10^5$ s⁻¹. To elucidate the mechanisms of this system, one has to take into account that under these experimental conditions, as shown earlier, linoleate peroxy radicals are produced within less 10 μs. In addition to the formation of linoleate peroxy radicals, HO₂[•] is also produced according to reaction $\text{H}^\bullet + \text{O}_2 \rightarrow \text{HO}_2^\bullet$. Because the pK_a of HO₂[•] is 4.7, it is expected that at pH 9.7 there is fast dissociation to form H⁺ + O₂^{•-}. We therefore attribute the fast component of the decay to the production of HO₂[•] and its consequent decay. It should be mentioned that O₂^{•-} disappearance cannot be followed by pulse radiolysis techniques because it is very slow in alkaline media [$2k(\text{O}_2^{\bullet-} + \text{O}_2^{\bullet-}) \sim 10^3$ L mol⁻¹ s⁻¹ at pH ~ 10].²⁷



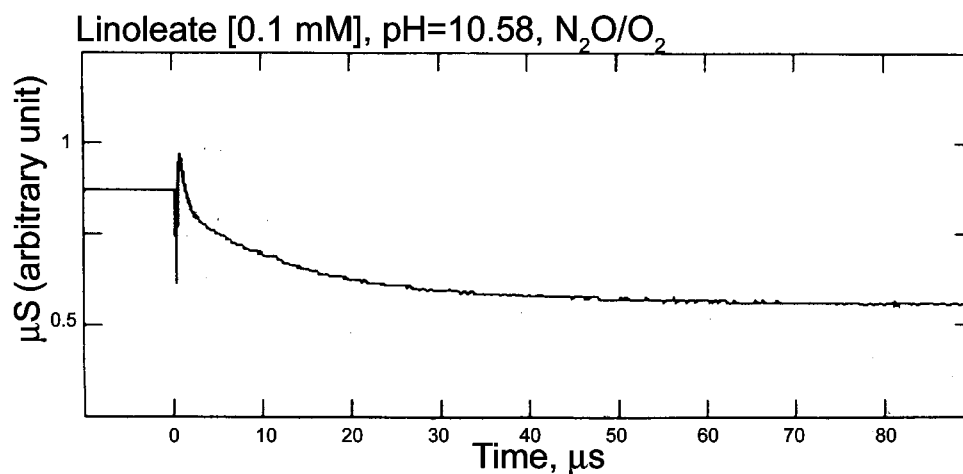
No HO₂[•]/O₂^{•-} elimination was observed (the absence of the slow component) in the pulsed irradiated aqueous solution of 0.1 mmol linoleic acid at pH ~ 3.

The second decay with a rate constant of $(6.0 \pm 0.9) \times 10^4$ s⁻¹ is much slower. At high dose per pulse, there is evidence that the elimination of HO₂[•]/O₂^{•-} is a base-catalyzed unimolecular reaction. One would postulate that the enhancement of higher pH on the O₂^{•-} elimination (reaction 16) involves a deprotonation process ($\text{O}_2\text{LH}_2\text{-OH} \rightarrow \text{O}_2\text{LH}_2\text{-O}^- + \text{H}^+$), followed by release of O₂^{•-}. As a result, in alkaline solutions, a decrease in the conductivity is expected, because the neutralization of H⁺ by the strongly conducting OH⁻ ($182 \Omega^{-1} \text{ cm}^2 \text{ equiv}^{-1}$ at 21 °C) is replaced by the less conducting O₂^{•-} ($65 \Omega^{-1} \text{ cm}^2 \text{ equiv}^{-1}$ at 21 °C) and linoleate anion with a ketone structure (reaction 15).

Arachidonate, linolenate, and oleate peroxy radicals have shown that they also undergo O₂^{•-} elimination reactions in pulsed irradiated solutions. Parts a–c of Figure 10 show typical conductivity changes in pulsed (50% N₂O + 50% O₂)-saturated solutions of arachidonate, linolenate, and oleate, respectively. As in the case of linoleate basic solution, the fast components in the decrease of the conductivity represent the neutralization reaction of H⁺ + OH⁻ followed by further slow components in the decrease of the conductivity, which demonstrate the unimolecular O₂^{•-} elimination reaction. As expected, parts a and b of Figure 10 show that the *G* value for the fast components (O₂^{•-}) is 0.056–0.06 because $G(\text{H}) = 0.06 \pm 0.006 \mu\text{mol J}^{-1}$. The $G(\text{O}_2^{\bullet-})$ values of the slow components, which represent



(a)



(b)

Figure 9. (a) Pseudo-first-order buildup at 245 nm in the pulsed irradiated (50% N_2O + 50% O_2)-saturated aqueous solutions of 0.1 mmol L^{-1} linoleate, at pH = 10.3 and dose rate of 14.8 Gy/pulse. (b) Conductivity change following a 30 ns pulse of 29 Gy in a (50% N_2O + 50% O_2)-saturated aqueous solutions of 0.1 mmol L^{-1} linoleate at pH \sim 10.

the $\text{O}_2^{\cdot-}$ elimination reactions of the fatty acid peroxy radicals, have higher values with arachidonic acid peroxy radicals and lower value with oleate acid peroxy radicals. At a dose rate of 80 Gy per 30 ns pulse, $G(\text{O}_2^{\cdot-})$ values for the slow component are as follows: arachidonate $0.23 \pm 0.023 \mu\text{mol J}^{-1}$; linolenate $0.14 \pm 0.014 \mu\text{mol J}^{-1}$; linoleate $0.07 \pm 0.007 \mu\text{mol J}^{-1}$; and less than 0.01 for oleate. These results show that the higher the number of double bonds, the greater are the G values of $\text{HO}_2^{\cdot}/\text{O}_2^{\cdot-}$ elimination reactions. At a higher degree of unsaturation, as in the case of linoleate, linolenate, and arachidonate, the production of $\cdot\text{OH}$ adduct peroxy radicals ($\cdot\text{O}_2\text{LH}_2\text{--OH}$) is

higher than the alkyl peroxy radical LHO_2^{\cdot} . As mentioned earlier, in the case of oleate, unlike linoleate, linolenic, and arachidonic acids, abstraction of H along the molecular chain by $\cdot\text{OH}$ is more predominant than the addition to the double bond, and subsequent LHO_2^{\cdot} formation.

We also investigated the unimolecular $\text{HO}_2^{\cdot}/\text{O}_2^{\cdot-}$ elimination reaction in linoleate rod-shaped micelle. Figure 11a shows the transient optical spectrum of the pulsed irradiation of (50% N_2O + 50% O_2)-saturated solutions of [20 mmol] linoleate at pH \sim 10.3. Unlike the pulsed irradiation (50% N_2O + 50% O_2)-saturated solutions of 0.1 mmol linoleate, where the linoleate

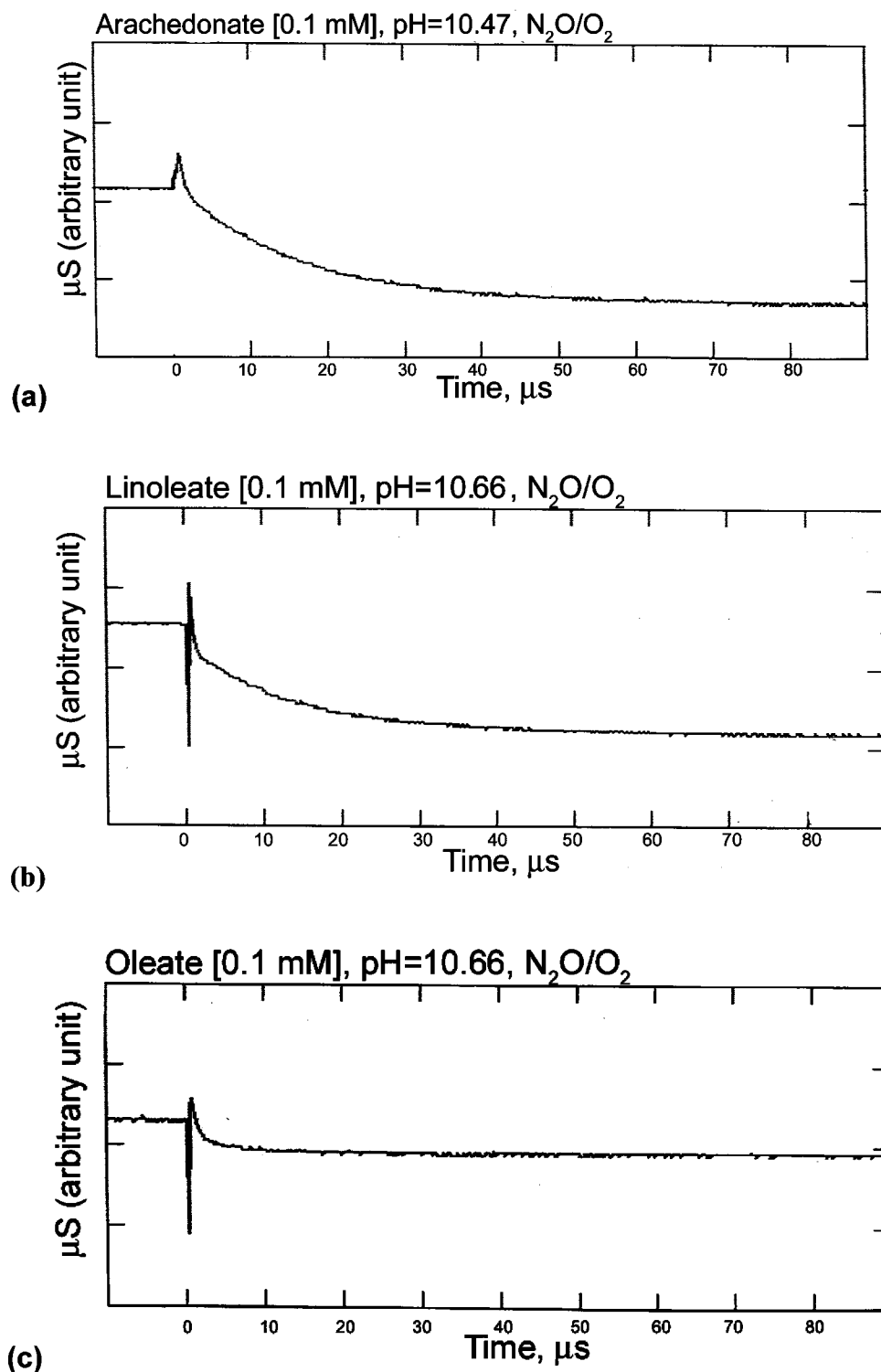


Figure 10. (a)–(c) Conductivity change following a 30 ns pulse of (50% N_2O + 50% O_2)-saturated aqueous solutions of 0.1 mmol L^{-1} arachidonate (a), 0.1 mmol L^{-1} linoleate (b), and 0.1 mmol L^{-1} oleate at pH ~ 10.3 –10.4.

molecules exist in monomeric form, at 20 mmol L^{-1} (Figure 11b) neither a small increase in the optical absorption at 245 nm nor a decrease was observed within 4 ms. Even with dose rates at 70–100 Gy per 20 ns pulse, to enhance the bimolecular decay of the peroxy radicals, no peroxy radical decay was observed at 245 nm within 500 ms. These results agree very well with published results showing that in micellar systems the abstraction reaction of allylic hydrogen by the peroxy radicals is predominant over the bimolecular peroxy decay.⁴ In addition, one would expect that the bimolecular decay in the

rod-shaped micelles is too slow to be measured by a pulse radiolysis apparatus with a 1 s maximum time scale. The small amount of the unimolecular $\text{HO}_2^*/\text{O}_2^{\bullet-}$ elimination reaction in the linoleate rod-shaped micelle is more difficult to elucidate. It has already been suggested that in aqueous alkaline linoleate micellar solutions, $\text{O}_2^{\bullet-}$ decays much faster, producing HO_2^* near the micellar surface.¹⁶ This suggestion stems from the much higher acidity at the electrical double-layer near the micelle surface, which significantly enhances the $\text{O}_2^{\bullet-} + \text{H}^+ \rightarrow \text{HO}_2^*$ reaction.

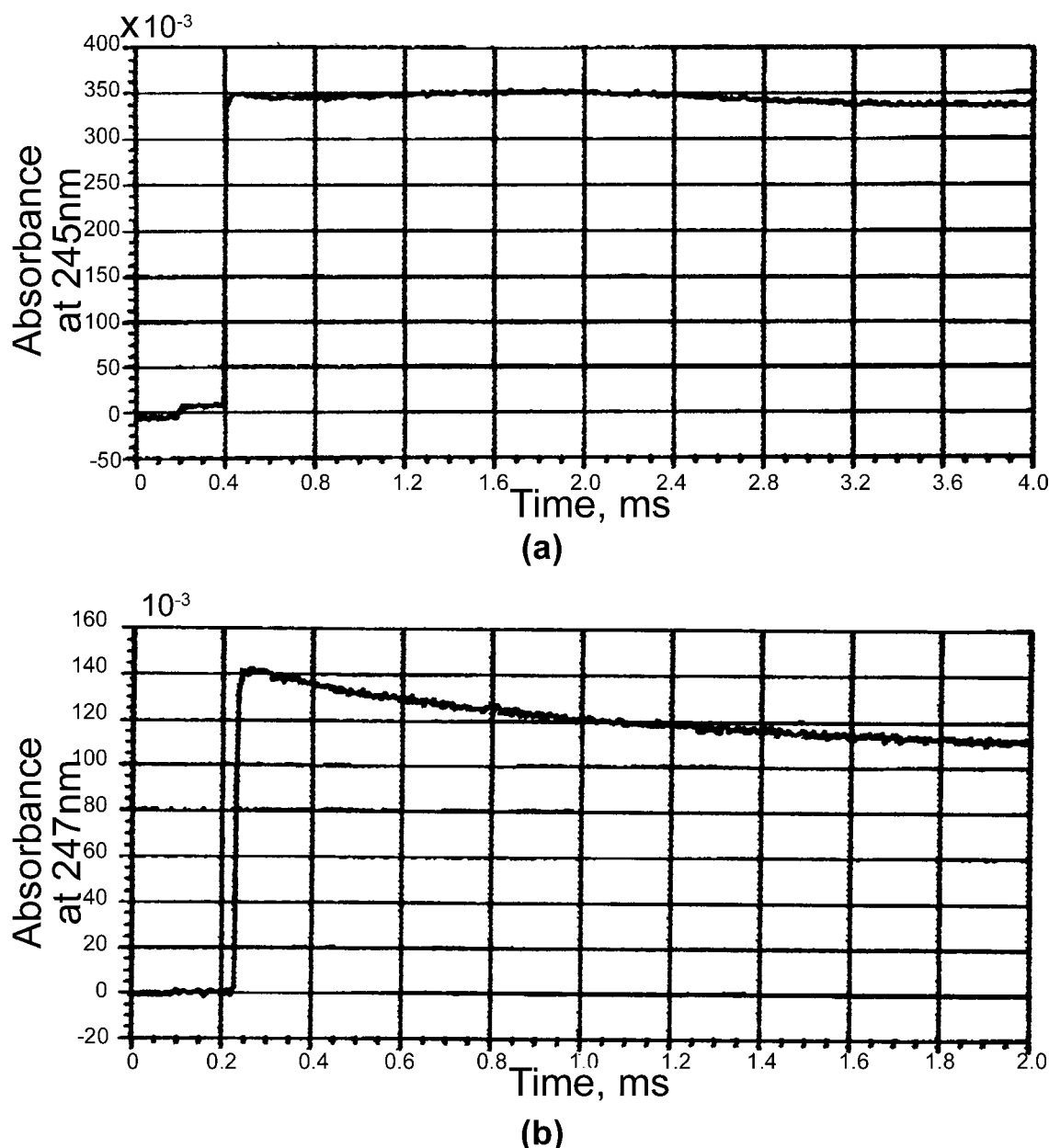


Figure 11. Comparison between the decay of the linoleate peroxy radicals at 245 nm in the rod-shaped micellar form 20 mmol L⁻¹, and in the monomeric aqueous form 0.1 mmol L⁻¹. (a) Time dependence of the absorption at 245 nm in the pulsed irradiated (50% N₂O + 50% O₂)-saturated solutions of 20 mmol L⁻¹ linoleate at pH \sim 10.3. Dose rate: 100 Gy per 20 ns pulse. (b) Time dependence of the absorption at 247 nm in the pulsed irradiated (50% N₂O + 50% O₂)-saturated solutions of 0.1 mmol L⁻¹ linoleate at pH \sim 9.7. Dose rate: 80 Gy per 20 ns pulse.

Concluding Remarks

This work shows that the overall allylic radical yield increases with the higher micelle structures due to the enhancement of the allylic abstraction inside the micelle. However, a higher dose rate decreases the allylic radical yield due to the increased rate of bimolecular reactions among radicals that are its immediate precursor; it also impedes the intramicellar abstraction of allylic hydrogen by linoleate molecules. This work also shows that the bimolecular decay reaction of allylic radicals are in the range 3–8 mmol L⁻¹; this can be explained by the occurrence of the open-ended self-association reactions of the linoleate molecules in the micellar system. We also demonstrate that the reaction rate constants of O^{•-} with the linoleate molecule decrease with increasing micellar structure because (1) the highly acidic character of the aqueous side of the electrical double layer near the micelle surface hinders the accessibility of the chain at higher micellar structure, and (2)

the repulsion of the negative charges between the O^{•-} and the carboxylic head of the linoleate.

In the presence of oxygen, using optical and conductometric methods, we show that the peroxy radicals derived from the OH adducts of oleate, linoleate, and arachidonate also undergo unimolecular HO₂[•]/O₂^{•-} elimination reactions. The yield of HO₂[•]/O₂^{•-} increases with decreasing dose rate and with increasing degree of unsaturation. However, no HO₂[•]/O₂^{•-} is observed in pulsed linoleate micellar solutions.

Acknowledgment. We thank Dr. Pedi Neta for valuable discussions and recommendations.

References and Notes

- (1) von Sonntag, C. *The Chemical Basis of Radiation Biology*; Taylor and Francis: London, 1987.
- (2) Erben-Russ, M.; Bors, W.; Saran, M. *Int. J. Radiat. Biol.* **1987**, *52*, 393–412.

- (3) Bors, W.; Erben-Russ, M.; Saran, M. *Bioelectrochem. Bioenerg.* **1987**, *18*, 37–49.
- (4) Porter, N. A. *Acc. Chem. Res.* **1986**, *19*, 262–268.
- (5) Gebicki, J. M.; Bielski, B. H. J. *J. Am. Chem. Soc.* **1981**, *103*, 7020–7022.
- (6) AlSheikhly, M.; Simic, M. G. *J. Phys. Chem.* **1989**, *98*, 3103–3106.
- (7) Katušin-Ražem, B.; Ražem, D. *J. Phys. Chem.* **2000**, *104*, 1482–1494.
- (8) Hunter, E. P. L.; Simic, M. G.; Michael, B. D. *Rev. Sci. Instrum.* **1985**, *56*, 2199–2204.
- (9) Maughin, R. L.; Michael, B. D.; Anderson, R. F. *Radiat. Phys. Chem.* **1978**, *11*, 229–.
- (10) Schuler, R. H.; Hartzell, A. L.; Behar, B. *J. Phys. Chem.* **1982**, *85*, 192–199.
- (11) Spinks, J. W. T.; Woods, R. J. *Radiation Chemistry*, 3rd ed.; John Wiley & Sons: New York, 1990.
- (12) Behar, D.; Czapski, G.; Duchovny, L. *J. Phys. Chem.* **1970**, *74*, 226.
- (13) Tabata, Y. *Pulse Radiolysis*; CRC Press: Boca Raton, FL, 1990.
- (14) Buxton, G. V.; Greenstock, C. L.; Helman, W. P.; Ross, A. B. *J. Phys. Chem. Ref. Data* **1988**, *17*, No. 2, 513.
- (15) Lindman, B.; Wennerstrom. Micelles. *Topics in Current Chemistry*; Springer-Verlag: Berlin, Heidelberg, New York, 1980.
- (16) Thomas, J. K. *The Chemistry of Excitation at Interface*; American Chemical Society: Washington, DC, 1984.
- (17) Patterson, L. K.; Hasegawa, K. *Ber. Bunsen-Ges., Phys. Chem.* **1978**, *82*, 951–958.
- (18) Neta, P.; Schuler, R. H. *J. Phys. Chem.* **1975**, *79*, 1–6.
- (19) Heijman, M. G. J.; Heitzman, A. J. P.; Nauta, H.; Levine, K. *Radiat. Phys. Chem.* **1985**, *26*, 83–88.
- (20) Sutherland, M. W.; Arudi, R. L.; Bielski, B. H. J. In *Oxy Radicals and Their Scavenger Systems*; Cohen, G., Greenwald, R. A., Eds.; Elsevier Biomedical: New York, 1983; Vol. 1, pp 266–269.
- (21) Pan, X.-M.; von Sonntag, C. *Z. Naturforsch.* **1990**, *45B*, 1337.
- (22) Rabani, J.; Kug-Roth, D.; Henglein, A. *J. Phys. Chem.* **1974**, *78*, 2089–2093.
- (23) Bothe, E.; Behrens, G.; Schulte-Frohlinde, D. *Z. Naturforsch.* **1977**, *32B*, 886–889.
- (24) Schuchmann, M. N.; Zegota, H.; von Sonntag, C. *Z. Naturforsch.* **1985**, *40B*, 215–221.
- (25) Schuchmann, M. N.; von Sonntag, C. *J. Chem. Soc., Perkin Trans. 2* **1993**, 289–297.
- (26) Al-Sheikhly, M. I.; Hissung, A.; Schuchmann, H. P.; Schuchmann, M. N.; von Sonntag, C.; Garner, A.; Scholes, G. *J. Chem. Soc., Perkin Trans. 2* **1984**, 601–608.
- (27) Bielski, H. J. *Photochem. Photobiol.* **1978**, *28*, 645–749.